# Mouse *limb deformity* mutations disrupt a global control region within the large regulatory landscape required for *Gremlin* expression

Aimée Zuniga,[1,2] Odyssé Michos,[1,2] François Spitz,[3] Anna-Pavlina G. Haramis,[4,5] Lia Panman,[2] Antonella Galli,[1] Kristina Vintersten,[4,6] Christian Klasen,[4] William Mansfield,[4] Sylwia Kuc,[2] Denis Duboule,[3] Rosanna Dono,[2,7] and Rolf Zeller[1,8]

[1]Developmental Genetics, Department of Clinical-Biological Sciences, University of Basel Medical School, CH-4056 Basel, Switzerland; [2]Department of Developmental Biology, Utrecht University, NL-3584CH Utrecht, The Netherlands; [3]Department of Zoology and Animal Biology, National Center of Competence in Research 'Frontiers in Genetics' University of Geneva, CH-1211 Geneva, Switzerland; [4]European Molecular Biology Laboratory, D-69117 Heidelberg, Germany

**The *mouse limb deformity* (*ld*) mutations cause limb malformations by disrupting epithelial–mesenchymal signaling between the polarizing region and the apical ectodermal ridge. *Formin* was proposed as the relevant gene because three of the five *ld* alleles disrupt its C-terminal domain. In contrast, our studies establish that the two other *ld* alleles directly disrupt the neighboring *Gremlin* gene, corroborating the requirement of this BMP antagonist for limb morphogenesis. Further doubts concerning an involvement of *Formin* in the *ld* limb phenotype are cast, as a targeted mutation removing the C-terminal Formin domain by frame shift does not affect embryogenesis. In contrast, the deletion of the corresponding genomic region reproduces the *ld* limb phenotype and is allelic to mutations in *Gremlin*. We resolve these conflicting results by identifying a *cis*-regulatory region within the deletion that is required for *Gremlin* activation in the limb bud mesenchyme. This distant *cis*-regulatory region within *Formin* is also altered by three of the *ld* mutations. Therefore, the *ld* limb bud patterning defects are not caused by disruption of *Formin*, but by alteration of a global control region (GCR) required for *Gremlin* transcription. Our studies reveal the large genomic landscape harboring this GCR, which is required for tissue-specific coexpression of two structurally and functionally unrelated genes.**

[*Keywords*: *cis* regulation; *Formin*; global control region; *Gremlin*; limb development; regulatory landscape]

The mouse is the genetic model of choice to study mammalian development and disease. In addition to alteration of specific genes by gene targeting and transgenesis, mutant mouse strains identified by phenotypic screens are commonly used to analyze developmental and disease processes (for reviews, see Justice 2000; Perkins 2002). A significant fraction of spontaneous mutations in mice (and humans) cause congenital limb malformations and have proven crucial to unravel the mo-

lecular mechanisms regulating vertebrate limb bud morphogenesis (for review, see Gurrieri et al. 2002). In particular, several alleles of the recessive mouse *limb deformity* (*ld*) mutation disrupt patterning of the distal limb skeleton. Over the years, a total of five *ld* alleles have been identified by phenotypic and genetic complementation analysis. All *ld* homozygous newborn mice display limb patterning defects characterized by synostosis of the zeugopod in combination with oligo- and syndactyly of metacarpal bones and digits (for review, see Zeller et al. 1999). In addition, *ld* homozygous newborn mice display varying degrees of uni- and bilateral renal aplasias depending on allele "strength" (Maas et al. 1994). Molecular analysis showed that the two *ld* alleles (*ld*[TgHd], *ld*[TgBri]) that arose by chance insertional mutagenesis disrupt the C-terminal region of the *Formin* gene (for details, see Wang et al. 1997). The *ld*[In2] allele arose by an ~40-Mb inversion with breakpoints in the C-ter-

Present addresses: [5]Hubrecht Laboratorium, NL-3584 CT Utrecht, The Netherlands; [6]Mount Sinai Hospital, Samuel Lunenfeld Research Institute, Stem Cell Mutagenesis Laboratory, Toronto, Ontario M5G 1X5, Canada; [7]Development and Pathology of the Nervous System, Institut de Biologie du Développement de Marseille Campus de Luminy, Case 907, F-13288 Marseille CEDEX 09, France.
[8]Corresponding author.
E-MAIL Rolf.Zeller@unibas.ch; FAX 41-16-267-3959.

Zuniga et al.

minal region of *Formin* and the *Agouti* locus (Maas et al. 1990; Woychik et al. 1990). To date the molecular lesions in the two first identified *ld* alleles, *ld*[OR] and *ld*[J] (for review, see Zeller et al. 1999), remained obscure as there are no alterations in the *Formin* open reading frame (ORF; Wynshaw-Boris et al. 1997). Formin (or *Formin-1*) is the founding member of a multigene family that mediates cytoskeletal rearrangements in response to signals that induce, for example, cell polarization (for review, see Evangelista et al. 2003). The Formin proteins are encoded by at least 24 exons spread over ~400 kb, and alternative splicing gives rise to several protein isoforms of ~180 kDa. All Formin isoforms share a proline-rich FH1 domain (interacting with SH3 domains and Profilin) and a highly conserved C-terminal FH2 domain, which is required to stimulate polymerization of linear actin filaments (for reviews, see Zeller et al. 1999; Kobielak et al. 2004). However, inactivation of specific Formin isoforms by gene targeting in the mouse resulted in partial renal agenesis phenotypes, but failed to reproduce the *ld* limb phenotype as limb morphogenesis was normal (Wynshaw-Boris et al. 1997; Chao et al. 1998).

In *ld* homozygous embryos, the epithelial–mesenchymal signaling interactions regulating limb bud development are disrupted (for review, see Panman and Zeller 2003). Limb bud growth and patterning are coordinately controlled by two main signaling centers, the *Sonic hedgehog* (*Shh*)-expressing polarizing region, located in the posterior limb bud mesenchyme and the apical ectodermal ridge (AER), which expresses several types of signals including *Fibroblast growths factors* (*Fgfs*) and *Bone morphogenetic proteins* (*Bmps*). Molecular analysis of *ld* mutant limb buds revealed that activation of *Fgf4* expression in the posterior AER, establishment of the SHH/FGF4 feedback loop, and thereby up-regulation of *Shh* expression by the polarizing region are disrupted (for review, see Panman and Zeller 2003). A functional screen for mesenchymal signals able to relay SHH to the AER resulted in identification of the BMP antagonist *Gremlin* as the signal lacking from *ld* mutant limb bud mesenchyme. Grafts of *Gremlin*-expressing cells into *ld* mutant limb buds restore *Fgf4* expression and the SHH/FGF4 feedback loop (Zuniga et al. 1999). Analysis of *Gremlin*-deficient mouse embryos generated by gene targeting has confirmed its essential functions during limb bud development (Khokha et al. 2003; Michos et al. 2004). Induction of *Fgf8*-expressing AER cells occurs normally, but a morphologically distinct and functional AER fails to form in *Gremlin*-deficient embryos. *Gremlin*-mediated BMP antagonism is required in the limb bud mesenchyme to enable expression of various types of AER signals such as *Fgfs* and *Bmps* and for survival of core mesenchymal cells (Michos et al. 2004). The general disruption of AER function in *Gremlin*-deficient embryos in turn blocks propagation of *Shh* expression by the polarizing region as is also observed in *ld* mutant limb buds. In addition, the induction of metanephric kidney organogenesis and complete differentiation of lung airway epithelia fail to occur, which causes neonatal lethality. The studies by Michos et al. (2004) reveal a more general role of *Gremlin*-mediated BMP antagonism in epithelial–mesenchymal signaling during vertebrate organogenesis. Interestingly, the *Gremlin* transcription unit maps only ~40 kb downstream from the *Formin* gene on mouse chromosome 2 and is transcribed in opposite orientation (University of California at Santa Cruz Genome Browser, http://genome.ucsc.edu). Finally, Khokha et al. (2003) established allelism between one of the *ld* alleles (*ld*[J]) and a *Gremlin* null allele generated by gene targeting, but did not analyze the genetic and molecular basis for these rather unexpected findings.

In the present study we establish that the *ld*[J] mutation is a point mutation affecting splicing of *Gremlin* transcripts that results in truncation of the 5′ part of the *Gremlin* ORF. Furthermore, the complete *Gremlin* ORF encoded by exon 2 is deleted by the *ld*[OR] mutation. Therefore, these two *ld* alleles are spontaneous *Gremlin* loss-of-function alleles, which also establishes that the *ld* complementation group encompasses both the *Gremlin* and *Formin* loci. Using gene targeting we show that disruption of the *Formin* FH2 domain by deleting coding exon 10 (*Fmn*[Δ10] mutation) does not reproduce the *ld* phenotype. In contrast, deletion of the genomic region encompassing exons 10–24 (*Fmn*[Δ10.24] mutation) results in the characteristic *ld* limb phenotype. Interestingly, the *Fmn*[Δ10.24] deletion, but not the *Fmn*[Δ10] mutation, is allelic to *Gremlin* loss-of-function mutations. Further analysis establishes that the deleted region encodes regulatory elements required to activate both *Formin* and *Gremlin* expression in the posterior limb bud mesenchyme and mediate responsiveness to SHH, but not to FGF signaling. BAC transgenic analysis positively identifies this *cis*-regulatory region and shows that it is required to activate *Gremlin* transcription in the posterior–distal limb bud mesenchyme. The features of this large *cis*-regulatory landscape are reminiscent of a recently discovered global control region, a novel type of chromosomal regulatory element that controls expression of 5′*Hoxd* genes in the distal limb bud mesenchyme (Spitz et al. 2003). Taken together, our studies establish that the *ld* limb phenotype is a direct consequence of losing *Gremlin* expression in the limb bud mesenchyme and not due to disrupting *Formin* functions. We also discuss how such large regulatory landscapes that control tissue-specific coexpression of functionally unrelated genes may have arisen.

## Results

### The ld[J] and ld[OR] alleles are loss-of-function mutations directly disrupting the Gremlin gene products

In contrast to the three independent alleles of the mouse *ld* mutation that truncate *Formin* (see the introduction), no molecular alterations of the *Formin* ORF were identified for the *ld*[OR] and *ld*[J] alleles (Wynshaw-Boris et al. 1997). However, both these *ld* mutations are allelic to null mutations in the neighboring *Gremlin* gene (generated by gene targeting; Michos et al. 2004) as compound heterozygous mice display the characteristic *ld* limb

phenotype (Fig. 1A; Khokha et al. 2003). Furthermore, newborn *ld*[OR] homozygous mice lack kidneys and ureters (Supplementary Fig. 1) similar to *Gremlin*-deficient and *ld*[J] homozygous mice (Maas et al. 1994). This renal agenesis in combination with lung defects (Supplementary Fig. 1) causes death shortly after birth identical to *Gremlin* null mutant mice (Michos et al. 2004). Molecular analysis of the *ld*[OR] allele indeed reveals a 12.7-kb genomic deletion removing the complete *Gremlin* ORF (Fig. 1B,C), which establishes the *ld*[OR] mutation as a spontaneous *Gremlin* null allele. In sharp contrast, *Gremlin* transcripts remain expressed in embryos homozygous for the *ld*[J] allele (Fig. 1D), despite the fact that activation of *Fgf4* in the posterior AER is disrupted and the *Shh* expressing polarizing region is not maintained (Haramis et al. 1995). Sequence analysis of the *Gremlin* locus in the *ld*[J] allele reveals a specific G-to-A base change at the first intron–exon 2 boundary (asterisk in Fig. 1E). This point mutation eliminates the intronic AG motif at the 3′ splice site, which is essential for correct pre-mRNA splicing (Faustino and Cooper 2003). Indeed, a single aberrantly spliced transcript with a 65-base deletion removing the 5′ part of exon 2 was identified in *ld*[J] homozygous embryos (Fig. 1F; data not shown). This aberrant splice makes use of a downstream AG dinucleotide within exon 2 that is preceded by a pyrimidine-rich stretch required for splicing (Fig. 1F; Faustino and Cooper 2003). This deletion within the *Gremlin* transcript removes the AUG translational start codon,

thereby abolishing translation of full-length secreted *Gremlin* protein (Fig. 1F).

### Not the disruption of the Formin FH2 domain, but deletion of the corresponding genomic region causes the ld limb phenotype

The fact that the *ld*[OR] and *ld*[J] alleles are *Gremlin* loss-of-function mutations (Fig. 1) reiterates the question of whether the disruption of *Formin* functions is indeed the primary cause of the *ld* phenotype. In particular, the *Gremlin* gene is located ~40 kb downstream from *Formin* and transcribed in opposite orientation, extending the *ld* complementation group to ~450–500 kb in size (Fig. 2A). Previous analysis showed that the other three *ld* alleles (*ld*[In2], *ld*[TgBri], and *ld*[TgHd]; for details, see Wang et al. 1997) disrupt the genomic region encoding the C-terminal part of *Formin* (encoded by exons 10–24; Fig. 2A). In an attempt to reproduce the *ld* phenotype and possibly generate a null allele by reverse genetics, *Formin* exon 10 was deleted (*Fmn*[Δ10] allele; Fig. 2B; for details, see Materials and Methods). Exon 10 was chosen as its deletion results in a frame shift that disrupts translation of the C-terminal protein domain completely (Fig. 2E). Rather unexpectedly, *Fmn*[Δ10] homozygous mice are phenotypically wild type (Fig. 2C; data not shown), thereby establishing that deletion of exon 10 is not sufficient to reproduce the *ld* phenotype. Next, we deleted the complete genomic region spanning exons 10–24 (Fig.
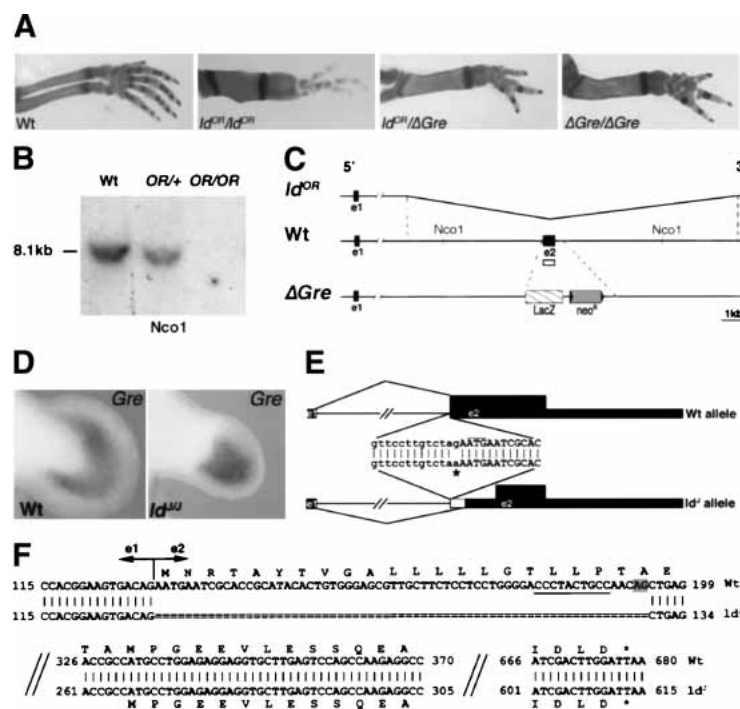


**Figure 1.** The *ld*[OR] and *ld*[J] mutations are *Gremlin* loss-of-function alleles. (*A*) The *ld*[OR] mutation is allelic to a *Gremlin* null allele (ΔGre) generated by gene targeting (Michos et al. 2004). (*B*) Southern blot analysis reveals that the *Gremlin* ORF encoded by exon 2 is deleted in the *ld*[OR] mutation. Genomic DNA isolated from embryos was digested by Nco1 and probed with a *Gremlin* exon 2 probe (open box in scheme, *C*). (Wt) Wild-type littermate; (*OR/+*) heterozygous embryo; (*OR/OR*) homozygous embryo. (*C*) Schematic representation of the *Gremlin* locus on chromosome 2 in the *ld*[OR] allele, wild-type, and ΔGre mutation. (*ld*[OR]) Kinked line indicates the 12.7-kb region deleted in the *ld*[OR] mutation. (Wt) Open box indicates the probe used for the Southern blot analysis shown in *B*. (ΔGre) *LacZ* and the *Neo*[R] replace coding exon 2 in the *Gremlin* null allele generated by gene targeting. (e1) Exon 1; (e2) exon 2. (*D*) *Gremlin* remains expressed in *ld*[J] homozygous embryos. Shown are limb buds of a wild-type (Wt) and *ld*[J] homozygous (*ld*[J/J]) mouse embryo at E11.5. (*E*) The G-to-A mutation at the intron–exon 2 junction of the *Gremlin* gene in the *ld*[J] allele (indicated by an asterisk) disrupts splicing. Lowercase indicate intronic, uppercase indicate exonic sequences. Thick black boxes indicate the *Gremlin* ORF, thin boxes indicate the 5′ and 3′ noncoding regions. The thin white box indicates the deletion of mRNA due to aberrant splicing. Thin black lines indicate intronic sequences and splices. (*F*) Aberrant pre-mRNA splicing deletes the first 65 bases of the *Gremlin* ORF. Shown is an alignment of the cDNA sequences of wild-type (Wt) and *ld*[J] alleles with the respective ORFs. The truncated *ld*[J] *Gremlin* transcript could potentially encode a *Gremlin* protein of 117 amino acids (instead of 184) lacking the signal peptide (Avsian-Kretchmer and Hsueh 2003). The AG dinucleotide used for splicing in the *ld*[J] allele is shaded gray. The required upstream poly-pyrimidine tract is underlined (Faustino and Cooper 2003).

**Figure 2.** Not disruption of the *Formin* FH2 domain, but deletion of the corresponding genomic region causes the *ld* limb phenotype. (*A*) Schematic representation of the *ld* complementation group consisting of *Formin* and *Gremlin* loci. The *Formin* gene is encoded by at least 24 exons (transcriptional direction indicated by arrow; Wang et al. 1997), whereas the *Gre* gene is transcribed in reverse orientation (bold arrow) and contains only two exons. The intergenic region separating the two genes is ~38 kb. The Formin FH2 domain is encoded by exons 10–24 and is present in all Formin protein isoforms (Wang et al. 1997). The following genetically engineered mutations are indicated: ($\Delta$10) $Fmn^{\Delta 10}$ allele; ($\Delta$10.24) $Fmn^{\Delta 10.24}$ allele; ($\Delta Gre$) $Gre^{\Delta ORF}$ null allele (Michos et al. 2004). The spontaneous *ld* alleles are indicated: ($ld^{TgBri}$) transgene induced deletion of genomic region between exons 19 and 23 (Vogt et al. 1992); ($ld^{TgHd}$) transgene insertional mutagenesis (Woychik et al. 1985); ($ld^{In2}$) 40-Mb inversion involving *Formin* and *Agouti* loci (Woychik et al. 1990); ($ld^{OR}$) deletion of the *Gre* ORF; ($ld^J$) point mutation disrupting *Gre* pre-mRNA splicing. (*B*) Schematic representation of the genetically engineered $Fmn^{\Delta 10}$ and $Fmn^{\Delta 10.24}$ alleles. (Neo) PGK-$Neo^R$ gene used to select ES-cell clones (first round of gene targeting); (Hygro) PGK-$Hygro^R$ gene used to select ES-cell clones (second round of gene targeting); (lacZ) IRES-*LacZ* gene used to tag *Fmn* transcripts. Arrows indicate direction of transcription. *Formin* exons are numbered as in *A*. (*C*, *left* panels) Limb skeletal phenotypes of wild-type and homozygous mice. Genotypes are indicated in the panels. (*Right* panels) Gremlin expression in limb buds of wild-type and homozygous embryos (E10.75). For nomenclature see the legend for *A*. (*D*) RT–PCR of *Formin* transcripts isolated from wild-type



(Wt), $Fmn^{\Delta 10}$ ($\Delta$10) and $Fmn^{\Delta 10.24}$ ($\Delta$10.24) homozygous embryos. Wild-type and $Fmn^{\Delta 10}$ mRNAs extending downstream from exon 9 were detected using primers in exons 9 and 23, $Fmn^{\Delta 10.24}$ mRNAs extending downstream from exon 9 were detected using primers in exon 9 and the IRES-*LacZ* tag (see Materials and Methods). (+) Reverse transcriptase included; (–) reverse transcriptase omitted (control). Note that the difference in size between wild-type (Wt) and $Fmn^{\Delta 10}$ transcripts is 150 bases, as expected. (*E*) Amino acid sequence deduced from the sequences of the *Formin* transcripts arising from wild-type, $Fmn^{\Delta 10}$ and $Fmn^{\Delta 10.24}$ alleles.

2A; region 10.24), which results in the $Fmn^{\Delta 10.24}$ allele (Fig. 2B; for details, see Materials and Methods). Mice homozygous for the $Fmn^{\Delta 10.24}$ allele indeed display the characteristic *ld* limb phenotype (Fig. 2C). However, $Fmn^{\Delta 10.24}$ homozygous newborn mice display neither renal agenesis nor lung patterning phenotypes and survive to adulthood (data not shown). Molecular analysis of $Fmn^{\Delta 10.24}$ homozygous embryos reveals that *Gremlin* expression is lost specifically from the limb bud mesenchyme, whereas it is normal in $Fmn^{\Delta 10}$ homozygous embryos (Fig. 2C; data not shown). In agreement with limb bud specific loss of *Gremlin* expression, activation of *Fgfs* in the posterior AER and SHH–GRE/AER feedback

signaling are disrupted in $Fmn^{\Delta 10.24}$ homozygous embryos (Supplementary Fig. 2), but not in $Fmn^{\Delta 10}$ homozygous embryos (data not shown). One possible explanation for the lack of an *ld* limb phenotype in $Fmn^{\Delta 10}$ homozygous embryos could be the rescue of *Formin* function due to aberrant splicing. However, thorough analysis of *Formin* transcripts extending 3′ to exon 9 by RT–PCR provided no evidence for aberrant splicing (Fig. 2D; data not shown). Furthermore, sequence analysis of the altered *Formin* transcripts in $Fmn^{\Delta 10}$ and $Fmn^{\Delta 10.24}$ homozygous embryos establishes that the *Formin* ORF is truncated in both alleles at the level of the exon 9/10 boundary (Fig. 2E). These results show that the *ld* limb
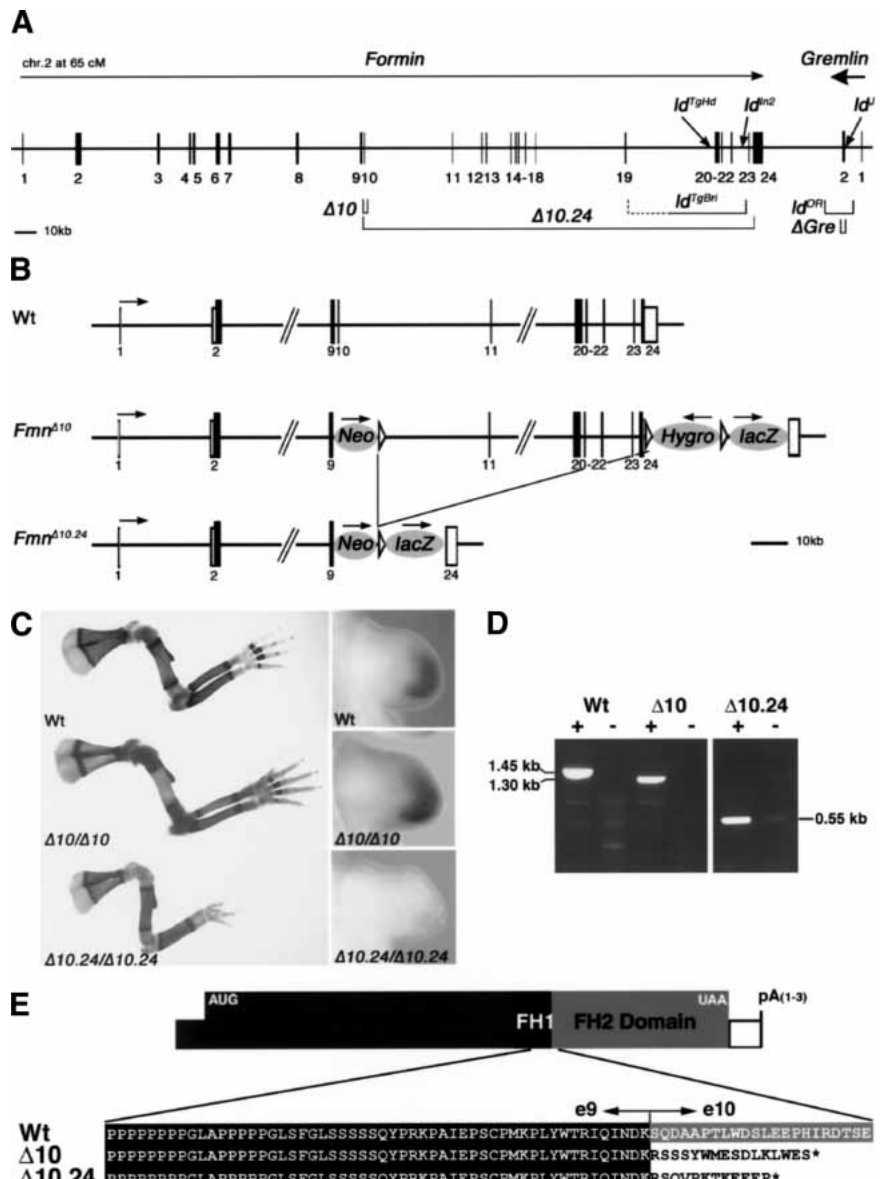
phenotype in the $Fmn^{\Delta 10.24}$ mutation is not caused by disruption of the C-terminal *Formin* protein domain as previously concluded (for review, see Zeller et al. 1999), but by the deletion of other essential elements located in the genomic region 10.24.
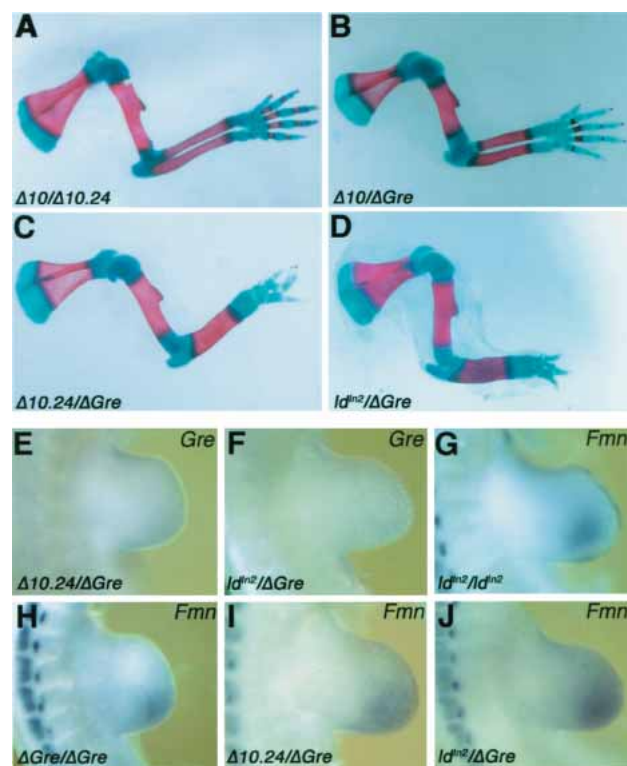
*The genomic region 10.24 exerts* cis-*effects on* Gremlin *expression in the limb bud mesenchyme*

The phenotypic analysis indicated that all *ld* mutations belong to the same complementation group in spite of their disrupting either the *Formin* or *Gremlin* loci (Fig. 2A); therefore, allelism between the $Fmn^{\Delta 10}$, $Fmn^{\Delta 10.24}$, and $Gre^{\Delta ORF}$ mutations was assessed. Limbs of $Fmn^{\Delta 10/\Delta 10.24}$ and $Fmn^{\Delta 10}$; $Gre^{\Delta ORF}$ compound heterozygous mice are normal (Fig. 3A,B), confirming the wild-type phenotypic nature of the $Fmn^{\Delta 10}$ mutation. In contrast, the $Fmn^{\Delta 10.24}$ mutation is a hypomorphic allele of the $Gre^{\Delta ORF}$ null mutation as $Fmn^{\Delta 10.24/+}$; $Gre^{\Delta ORF/+}$ mice display a fully penetrant *ld* limb phenotype (Fig. 3C), but not the phenotypes causing neonatal lethality (data not



**Figure 3.** The $Fmn^{\Delta 10.24}$ and $ld^{In2}$ mutations are allelic to $Gre^{\Delta ORF}$ by disrupting *cis* regulation of *Gremlin* in the limb bud mesenchyme. (*A–D*) Forelimb skeletal phenotypes of compound heterozygous mice. (*E,F*) *Gremlin* is no longer expressed in the limb bud mesenchyme of $Fmn^{\Delta 10.24/+}$; $Gre^{\Delta ORF/+}$ (*E*) and $ld^{In2/+}$; $Gre^{\Delta ORF/+}$ (*F*) compound heterozygous embryos. (*G–J*) *Formin* remains expressed in the limb bud mesenchyme of $ld^{In2/In2}$ (*G*), $Gre^{\Delta ORF/\Delta ORF}$ (*H*), $Fmn^{\Delta 10.24/+}$; $Gre^{\Delta ORF/+}$ (*I*), and $ld^{In2/+}$; $Gre^{\Delta ORF/+}$ (*J*) compound heterozygous embryos. Note: Samples *G–J* were pretreated prior to whole mount in situ hybridization for optimal detection of *Formin* transcripts in the mesenchyme. Such pretreatment results in loss of the AER. Genotypes are indicated as defined in the legend for Figure 2A.
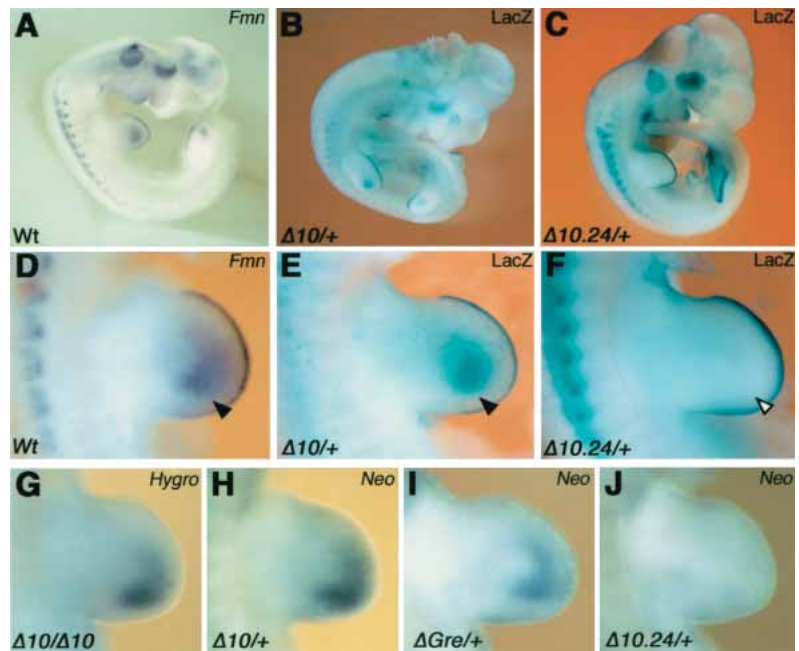
shown). The $ld^{In2}$ allele is of particular interest, as an inversion between *Formin* and *Agouti* (Woychik et al. 1990) relocates the *Gremlin* gene ~40 Mb away on mouse chromosome 2. Compound $ld^{In2/+}$; $Gre^{\Delta ORF/+}$ heterozygous mice also display the *ld* limb phenotype (Fig. 3D), which indicates that integrity of the genomic region encoding *Formin* and *Gremlin* (Fig. 2A) is required in *cis* for normal limb bud development. Therefore, the loss of *Gremlin* expression in $Fmn^{\Delta 10.24}$ (Fig. 2E) and $ld^{In2}$ homozygous limb buds seems to be a consequence of either deleting ($Fmn^{\Delta 10.24}$) or disrupting ($ld^{In2}$) a distant *cis*-regulatory element of *Gremlin* expression in limb buds rather than disrupting *Formin* functions (Zuniga et al. 1999). Indeed, *Gremlin* transcription is lost from the limb bud mesenchyme of $Fmn^{\Delta 10.24}$; $Gre^{\Delta ORF}$ and $ld^{In2}$; $Gre^{\Delta ORF}$ compound heterozygous embryos (Fig. 3E,F). Conversely, *Formin* remains expressed in limb buds of $ld^{In2}$ and $Gre^{\Delta ORF}$ homozygous (Fig. 3G,H) and compound heterozygous embryos (Fig. 3I,J). These results indicate that the relevant elements in question are located upstream of *Formin* coding exon 23. As no additional genes have been found in the genomic region 10.24 (data not shown), these results indicate that this region is required for *cis* regulation of *Gremlin* expression in the limb bud mesenchyme.

*Cis-regulatory elements in region 10.24 mediate activation and SHH responsiveness in the limb bud mesenchyme*

To explore the molecular mechanism for *cis* regulation of *Gremlin*, we analyzed the expression of exogenous genes inserted into the *ld* locus (Fig. 2A,B). In the $Fmn^{\Delta 10}$ and $Fmn^{\Delta 10.24}$ alleles, expression of the *LacZ* reporter gene is controlled by the endogenous *Fmn* promoters (Fig. 2B). As a consequence, the *LacZ* distribution recapitulates *Formin* expression perfectly in $Fmn^{\Delta 10}$ heterozygous embryos (Fig. 4, cf. A and B). In $Fmn^{\Delta 10.24}$ heterozygous embryos, *LacZ* activity (Fig. 4C) is specifically lost from the limb bud mesenchyme (arrowheads in Fig. 4, cf. D,E and F). These results reveal that the genomic region 10.24 is required for limb bud mesenchymal expression of both *Gremlin* and *Formin* (Figs. 3E, 4C,F). Furthermore, insertion of PGK promoters driving expression of $Neo^R$ and $Hygro^R$ genes at various positions (Fig. 2B) results in these exogenous transcripts being expressed like *Formin* and *Gremlin* in the limb bud mesenchyme (Fig. 4G–I), irrespective of transgene insertion site and orientation (Fig. 2B). In contrast, expression of the $Neo^R$ transgene is lost in limb buds heterozygous for the $Fmn^{\Delta 10.24}$ mutation (Fig. 4J). These results reveal the presence of *cis*-regulatory elements within *Fmn* genomic region 10.24 able to drive expression of exogenous genes in the limb bud mesenchyme. As both *Gremlin* and *Formin* expression are positively regulated by SHH signaling in the limb bud mesenchyme (Zuniga et al. 1999), a potential role of region 10.24 in mediating this SHH responsiveness was assessed. Indeed, anterior grafts of SHH expressing cells induce ectopic *LacZ* expression in cultured limb buds of $Fmn^{\Delta 10}$ heterozygous embryos

Zuniga et al.



**Figure 4.** The *Formin* genomic region 10.24 regulates expression of endogenous and exogenous transcription units inserted into the *ld* locus. (*A*) *Formin* transcript distribution in a wild-type embryo around gestational day 10.5 (hemisection). (*B*) *LacZ* recapitulates the *Formin* transcript distribution in the $Fmn^{\Delta10}$ allele. (*C*) Limb bud mesenchymal *LacZ* is specifically lost in the $Fmn^{\Delta10.24}$ allele. (*D*–*F*) Forelimb buds of the embryos shown in *A*–*C*. Black arrowheads indicate *Fmn/LacZ* distribution in the mesenchyme and open arrowhead indicates the loss of *LacZ* in the $Fmn^{\Delta10.24}$ allele. (*G*–*J*) Limb bud mesenchyme-specific expression of the $Hygro^R$ (*G*) and $Neo^R$ (*H*–*J*) genes inserted into the *ld* locus. Genotypes are indicated as defined in the legend for Figure 2A.

(Fig. 5, cf. A and B). In contrast, SHH is unable to induce *LacZ* expression in limb buds of $Fmn^{\Delta10.24}$ heterozygous embryos (Fig. 5, cf. C and D), which indicates that this region participates in mediating SHH responsiveness of *Formin* and *Gremlin* in the limb bud mesenchyme. In contrast to the $Fmn^{\Delta10.24}$ allele (Fig. 5D), *Formin* but not *Gremlin* (Zuniga et al. 1999) expression can be ectopically induced by SHH in $ld^{In2}$ homozygous limb buds (Fig. 5, cf. E and F; data not shown). These results show that the inversion affecting the $ld^{In2}$ allele separates the *Gremlin*, but not *Formin* transcription unit from the SHH response elements (see also Fig. 7A, below).

Analysis of *Gremlin* expression in chicken embryos suggested that its expression in the limb bud mesenchyme may depend on FGF signaling by the AER (Merino et al. 1999). However, limb buds of $Fmn^{\Delta10/\Delta10}$ embryos cultured in the presence the FGF signaling inhibitor SU5402 (Mohammadi et al. 1997; for details, see Materials and Methods) continue to express *LacZ* and *Gremlin* (Fig. 5, cf. G,I and H,J). As expected, inhibition of FGF signaling causes flattening of the AER (data not shown) and subsequent down-regulation of *Shh* and *Fgf* expression due to disrupting feedback signaling (Fig. 5K,L; data not shown). The results shown in Figure 5G–J indicate that mesenchymal *Formin* and *Gremlin* expression does not depend significantly on FGF signaling. In agreement, genetic analysis reveals that *Gremlin*, but not *Shh*, remains expressed in mouse limb buds lacking both *Fgf8* and *Fgf4* (Sun et al. 2002).

*The genomic region 19.23 is sufficient to activate gene expression in the limb bud mesenchyme*

Using a BAC-based strategy to generate transient transgenic mouse embryos, we have positively identified the

relevant *cis*-regulatory region (Fig. 6). Initially, a BAC containing the mouse *Fmn* genomic region spanning exons 19–24, the intergenic region, and the complete *Gremlin* transcription unit (tagged by *LacZ* in exon 2) was injected into fertilized oocytes and embryos stained for *LacZ* activity during gestational days 10.5 (Fig. 6A). This transgene (BAC construct A) is expressed in the posterior limb bud mesenchyme (arrowheads in Fig. 6A, n = 5/6), which indicates that all the required *cis*-regulatory elements are present. In contrast, *LacZ* activity is specifically lost from the limb bud mesenchyme of embryos harboring BAC construct B, which lacks region 19.23 (Fig. 6B, n = 7/7). The potential autonomy of region 19.23 (Fig. 6C) was assessed by inserting it downstream from a *LacZ* gene under control of a minimal β-globin promoter (Morgan et al. 1996). Indeed, BAC construct C (Fig. 6C) and a shorter construct containing region 20.23 (data not shown) are sufficient to drive *LacZ* expression into the posterior limb bud mesenchyme (Fig. 6C, arrowheads, n = 2/6). These results establish that region 19.23 encodes *cis*-regulatory elements sufficient to activate gene expression in combination with either the endogenous *Gremlin* or an exogenous minimal promoter (albeit with lower efficiency; Fig. 6, cf. A and C). Furthermore, region 19.23 is sufficient to activate *LacZ* expression in both dorsal and ventral posterior limb bud mesenchyme similar to *Formin* and *Gremlin* (Supplementary Fig. 3). Reduction of this genomic region reduces expression further, indicating that the required regulatory elements are spread over a larger region (see also Fig. 7; data not shown).

## Discussion

We establish that the *ld* phenotype is caused by disrupting either the regulatory landscape controlling transcrip-

tional activation of the BMP antagonist *Gremlin* in the limb bud mesenchyme or directly the *Gremlin* transcription unit. Therefore, the *ld* phenotype has been wrongly attributed to disruption of *Formin* functions. We now show that all *ld* alleles together with the $Fmn^{\Delta 10.24}$ and $Gre^{\Delta ORF}$ mutations define one allelic series of variable phenotypic strength. The $ld^{OR}$, $ld^{J}$, and $Gre^{\Delta ORF}$ alleles are the strongest alleles as the *Gremlin* gene products are either deleted or truncated, which causes a pleiotropic loss-of-function phenotype. The complete renal agenesis and lung septation defects in $ld^{OR}$ homozygous newborn mice result in fully penetrant neonatal lethality identical to the $Gre^{\Delta ORF}$ null allele generated by gene targeting (Michos et al. 2004). A second class of *ld* alleles is hypomorphic ($Fmn^{\Delta 10.24}$, $ld^{In2}$, $ld^{TgBri}$, $ld^{TgHd}$). These *ld* alleles display the characteristic and fully penetrant *ld* limb phenotype, but either lack or only show low frequencies of renal abnormalities and thereby generally survive to adulthood (see also Maas et al. 1994). A *cis*-regulatory region located within *Formin* that is required for *Gremlin* activation in the limb bud mesenchyme is either deleted or disrupted by all these hypomorphic *ld* alleles (Fig. 7A). Therefore, these mutations induce limb bud specific loss of *Gremlin* expression in *cis* and not in *trans* as a consequence of disrupting *Formin* (Zuniga et al. 1999). Despite the fact that $Fmn^{\Delta 10}$ homozygous mice (lacking the complete C-terminal Formin domain) are normal, it cannot be excluded that other Formin protein

domains function during embryonic development in pathways other than the ones disrupted due to the lack of the BMP antagonist *Gremlin*. In particular, specific inactivation of *Formin* isoform IV results in low penetrance and mostly partial renal agenesis phenotypes, whereas limbs are phenotypically wild type (Wynshaw-Boris et al. 1997; Chao et al. 1998). The partial disruption of kidney development in these mutations and some of the hypomorphic *ld* alleles (see before) correlate well with abundant *Formin* expression during kidney morphogenesis (for review, see Zeller et al. 1999).

Our studies reveal the molecular disruption of *Gremlin* in the $ld^{OR}$ and $ld^{J}$ alleles and positively identify the shared limb bud *cis*-regulatory elements in *Formin* genomic region 19.23. In particular, these latter studies explain satisfactorily why disruption of *Gremlin* functions is the primary cause of the limb phenotypes observed in *ld* homozygous mice. In the $ld^{In2}$ allele, the inversion between *Formin* and *Agouti* (Woychik et al. 1990) relocates the *Gremlin* gene ~40 Mb away from the genomic region 19.23 (Fig. 7A). The $ld^{TgHd}$ allele arose by insertion of multiple copies of a MMTV–myc transgene in combination with an ~1-kb deletion between *Formin* exons 19 and 20 (Woychik et al. 1985). The transgene insertion site disrupts the genomic region 19.23 and is likely to tether long-range-enhancing activity due to insertion of several strong exogenous promoters (Fig. 7A). Last but not least, the genomic region 19.23 is de-
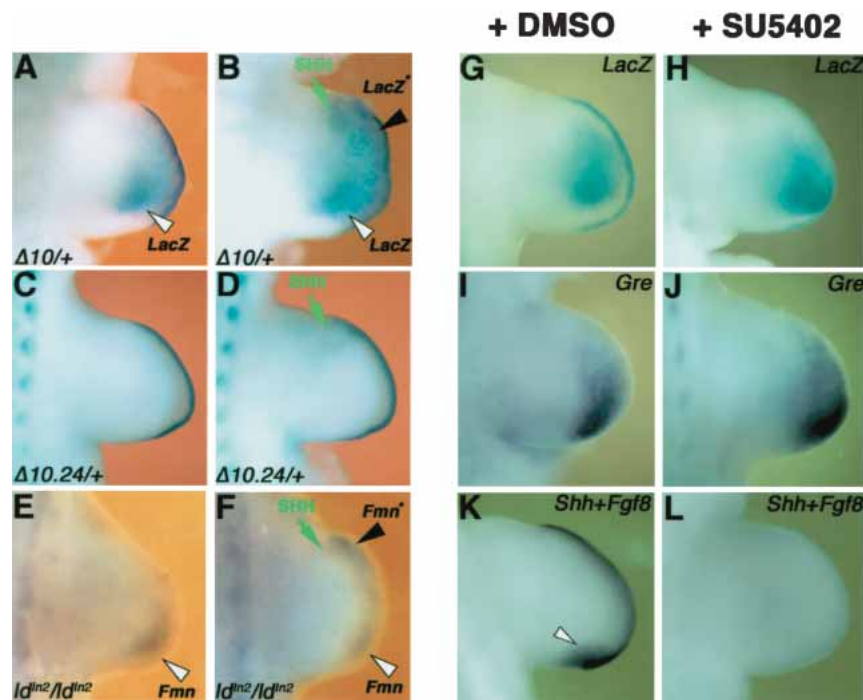


**Figure 5.** The limb bud regulatory region 10.24 is responsive to SHH signaling. SHH-expressing cells were grafted to the anterior limb bud mesenchyme (E10.25, 32–34 somites) and trunks cultured for 16–20 h prior to analysis. (*A*) Nongrafted limb bud of an $Fmn^{\Delta 10}$ heterozygous embryo (control). (*B*) Ectopic *LacZ* in the contralateral limb bud having received an anterior graft of SHH expressing cells. (*C*) Control $Fmn^{\Delta 10.24}$ heterozygous limb bud. (*D*) Failure to induce *LacZ* expression in response to SHH-expressing cells in an $Fmn^{\Delta 10.24}$ heterozygous limb bud. (*E*) Control limb bud of an $ld^{In2}$ homozygous embryo. (*F*) Induction of *Fmn* expression in response to ectopic SHH signaling in an $ld^{In2}$ homozygous embryo. In *A*–*F*, a green arrow indicates the position of SHH expressing cells, a black arrowhead and an asterisk indicate ectopic gene expression, and an open arrowhead indicates endogenous expression. (*G*–*L*) *Gremlin* and *Formin* expression are maintained in limb buds in which FGF signaling transduction has been blocked by the inhibitor SU5402. Forelimb buds of $Fmn^{\Delta 10/\Delta 10}$ embryos (E10.0, 29–32 somites) were cultured in the presence of 10 µM SU5402 (+SU5402; stock dissolved in DMSO) for 14–16 h prior to analysis. Controls were cultured in the presence of an equal concentration of DMSO (+DMSO; 0.03% final concentration in medium). (*G*) *LacZ* detection in an untreated limb bud. (*H*) *LacZ* remains in a limb bud cultured in the presence of SU5402. Note the down-regulation of *LacZ* in the AER due to flattening in the absence of FGF signal transduction. (*I*) *Gremlin* expression in an untreated limb bud. (*J*) *Gremlin* remains in a limb bud cultured in the presence of SU5402. (*K*) Detection of *Shh* (arrowhead) and *Fgf8* transcripts (AER) in an untreated limb bud. (*L*) Loss of both *Shh* and *Fgf8* expression in a limb bud cultured in the presence of SU5402.
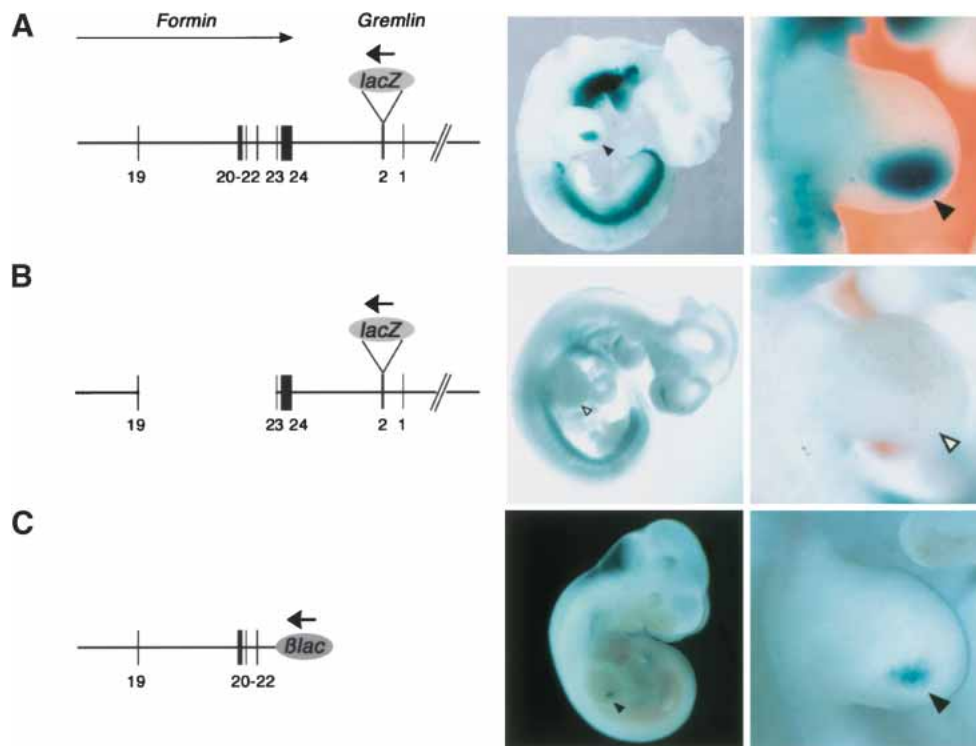
**Figure 6.** The *Fmn* locus encodes a regulatory region sufficient to activate *Gremlin* transcription in the limb bud mesenchyme. (*A*) Construct A was generated by in frame insertion of a *LacZ* gene 30 bases downstream from the *Gremlin* ATG (exon 2) into BAC #113H17. This BAC encodes *Fmn* exons 19–24, the intergenic region, entire *Gremlin* gene and extends ~150 kb upstream of *Gremlin* exon 1. Note that *Gremlin* (bold arrow) is transcribed in reverse orientation to *Formin* (arrow). (*B*) Construct B was generated by deleting the genomic region delimited by exons 19–23 from construct A. (*C*) Construct C was generated by replacing *Fmn* exon 23 and all downstream sequences with the β-*lac* reporter gene in BAC #113H17. Note that the β-*lac* reporter gene inserted in construct C is transcribed like *Gremlin*, that is, in reverse orientation (bold arrow) to *Formin*; exons are numbered as in Figure 2A. For all constructs, the *LacZ* distribution is shown in founder embryos around gestational day 10.5. *Left* panels show whole embryo views and *right* panels show forelimb buds. Note that different embryos are shown in the *left* and *right* panels. Black arrowheads point to the *LacZ* expression domains in the limb bud. Open arrowheads indicate the lack of *LacZ* expression in the limb bud of an embryo transgenic for construct B.

leted in the *ld*[TgBri] allele (Vogt et al. 1992). We establish that such a deletion completely abolishes *Gremlin* activation in the posterior limb bud mesenchyme (Fig. 7A). Our results also reveal the need to reexamine the human congenital malformations mapping to the orthologous locus on chromosome 15q13-14 (Maas et al. 1991) with phenotypes similar to *limb deformity*. Despite the fact that mutations in the *Gremlin* and *Formin* ORF have been excluded (Bacchelli et al. 2001; Morgan et al. 2003), mutations in the homologous *cis*-regulatory elements may cause these malformations.

The positively identified *cis*-regulatory region 19.23 (Fig. 7A) activates transcription of unrelated genes in a promoter- and orientation-independent manner at large distances. These features are strikingly similar to the ones of a recently identified global control region (GCR), which regulates limb bud specific expression of 5′*Hoxd* and the unrelated *Evx2* and *Lunapark* (*Lnp*) genes (Spitz et al. 2003). Such GCRs seem to consist of multiple regulatory regions and/or enhancers that form a chromosomal regulatory landscape and act at a distance to co-activate sets of neighboring genes in specific tissues.

Comparison of the orthologous mouse and human genomic regions 19.23 reveals highly conserved sequences within introns (at least 100 bases with more than 75% identity) that are spread over the whole region (Fig. 7B). However, no obvious consensus binding sites for, for instance, GLI transcription factors have been found within these conserved blocks (F. Spitz, unpubl.).

Interestingly, neither *Lnp* nor *Formin* are essential for limb development in spite of these loci harboring the essential GCR and being expressed during limb bud development. *Cis* regulation of the further downstream 5′*Hoxd* and *Gremlin* genes by the GCR is however essential for distal limb bud morphogenesis (Zákány and Duboule 1996; Khokha et al. 2003; Michos et al. 2004). Experimental evidence indicates that the *Formin* landscape region 10.24 not only contains the regulatory elements necessary for activation, but also the ones mediating response to SHH signaling (Fig. 7A). Regulation of these two genes in the limb bud mesenchyme is likely regulated by interaction of several control regions scattered over the genomic landscape (Fig. 7A,B). Our studies also reveal for the first time that such landscapes and GCRs are not a peculiar feature of regulating function-

ally related and clustered genes such as, for example, 5'*Hoxd* and globin genes (for review, see Zeller and Deschamps 2002). Rather, they seem to represent a novel mechanism by which tissue-specific coexpression of neighboring genes is orchestrated, even if they are structurally and functionally not related. These studies are likely to reveal the tip of the iceberg and further exploration of these regulatory landscapes will be necessary to understand if GCRs are composed of novel types of tissue-specific activator/enhancer elements or if they harbor elements enabling the known activators and enhancers to act over greater than usual distances (Fig. 7; Spitz et al. 2003). Last but not least, *Shh* expression in the limb bud mesenchyme is itself controlled by a regulatory region located ~800 kb upstream within the unrelated *Lmbr1* gene (Lettice et al. 2002).

It could well be that during evolution of vertebrates an initial selective constraint resulted in *Formin* and *Grem-*

*lin* being kept neighboring genes and their expression became coregulated as part of a larger regulatory landscape. In fact, both genes are also expressed in similar but not identical patterns during kidney organogenesis, and genetic analysis has revealed essential functions for both genes during kidney development (Wynshaw-Boris et al. 1997; Michos et al. 2004). Initial intertwining of their regulation could have resulted in them becoming inseparably linked or trapped into this regulatory landscape, in spite of eventual diversification of their functions during vertebrate evolution. The present study establishes that *Gremlin* and *Formin* are neither part of the same pathway nor a common synexpression group (Niehrs and Pollet 1999), in spite of these two genes being coexpressed in various embryonic tissues. Much of the gene diversity during vertebrate evolution is thought to have arisen following gene and chromosomal duplications. Interestingly, the arrangement of *Formin-2* (Leader
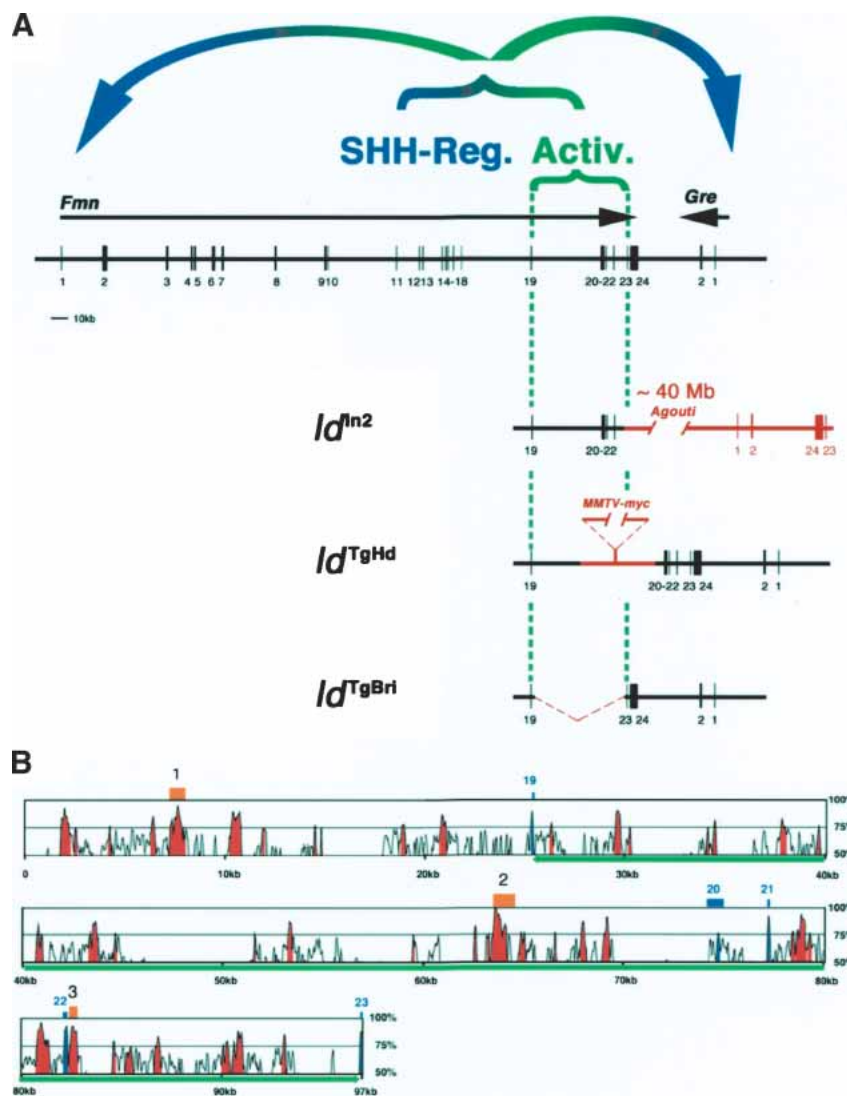


**Figure 7.** The large regulatory landscape required for activation of *Gremlin* expression in the limb bud mesenchyme. (*A*) Region 19.23 is disrupted by all relevant *ld* alleles. (Activ.) A global control region (GCR) located in the genomic region encompassing *Formin* exons 19–23 is required in *cis* for activation of *Gremlin* and *Formin* expression in the posterior limb bud mesenchyme. This region is disrupted in the *ld*[In2], *ld*[TgHd], and *ld*[TgBri] alleles. (SHH-Reg.) The region necessary for SHH-mediated regulation of *Gremlin* and *Formin* (see Fig. 5A–F) is most likely located upstream of *Formin* exon 19. Schemes show how the *ld*[In2], *ld*[TgHd], and *ld*[TgBri] mutations disrupt the activator GCR. (*B*) Alignment of the orthologous region 19.23 from the mouse and human genome using the mVISTA program (window size, 100 bases; homology threshold, 65%; Mayor et al. 2000). This alignment reveals multiple blocks of intronic sequences highly conserved between the two species. Exons 19–23 are indicated in blue and the parts of intronic sequences conserved more than 75% are marked as red peaks. The green line indicates the genomic sequences driving *LacZ* expression in BAC construct C (see Fig. 6C). The chicken genomic region 19.23 is only partially available, with some gaps in the regions containing the blocks of sequence conserved between mouse and human genome that precluded complete analysis. However, three regions (indicated in orange) highly conserved among all three species have been identified. Region 1 (upstream of exon 19): 77.4% identity over 243 bases. Region 2 (upstream of exon 20): 85.1% over 329 bases. Region 3 (just downstream from exon 22): 81% over 352 bases. The human, mouse, and chicken genomic sequences were obtained from the Ensembl Genome Browser (http://www.ensembl.org) using genome assembly releases v19.34b, v19.32.2, and prerelease1, respectively.

Zuniga et al.

and Leder 2000) and *Gremlin-2* (or *Prdc*; Minabe-Saegusa et al. 1998) on mouse chromosome 1 is identical to chromosome 2, as the two genes are also located next to one another and transcribed in reverse orientation (see also UCSC Genome Browser, http://genome.ucsc.edu). During organogenesis, both *Formin-2* and *Gremlin-2* are expressed in the developing neural tube (Minabe-Saegusa et al. 1998; Leader and Leder 2000), suggesting that they could also be part of a common regulatory landscape.

Large-scale phenotypic screens have become a renewed and major effort to genetically analyze vertebrate model organisms such as zebrafish and mouse (Justice 2000). Such screens provide powerful tools to identify the gene cascades controlling development, physiology, and disease by scoring for the relevant phenotypes. However, the present study reveals that in specific cases, the identification and analysis of the essential gene and/or cascades can be rather tedious. The molecular alterations in the *Formin* locus together with the *Formin* transcript and protein distribution established this gene as the obvious candidate, whose disruption causes the *ld* phenotype (for reviews, see Zeller et al. 1999; Panman and Zeller 2003). Only the combination of experimental embryology with advanced reverse genetics and transgenesis has finally revealed the true nature of the *ld* limb phenotype and established *Gremlin* as the essential one of the two disrupted genes. As many vertebrate genes contain rather large intronic and noncoding regions, such large regulatory landscapes may be rather common and more surprises with respect to assigning phenotypes to alterations of particular genes and/or pathways may well be in store.

## Materials and methods

### Mapping and identification of the ld^OR and ld^J mutations

The deletion of the *Gremlin* ORF in the $ld^{OR}$ allele was initially detected by Southern blotting (Fig. 1B) and mapped using a combination of Southern blot and long-range PCR analysis (Jansen et al. 1997). A PCR fragment spanning the deletion breakpoints in the $ld^{OR}$ allele was isolated. This fragment was sequenced and the extent of the deletion identified by sequence comparison to the wild-type *Gremlin* locus. The $ld^{OR}$ allele was crossed into 129S3/SvImJ, C57BL/6, and CD1 strains, as the penetrance of the kidney phenotype depends on genetic background. In the 129S and CD1 backgrounds, the kidney phenotype is fully penetrant (Supplementary Fig. 1). The point mutation affecting splicing of *Gremlin* in the $ld^J$ allele was identified as follows. Total RNAs were isolated from wild-type and $ld^{J/J}$ mouse embryos (embryonic day 12 [E12]) using the RNeasy kit (Qiagen) and cDNAs synthesized using standard procedures. *Gremlin* transcripts were amplified using specific primers in exons 1 and 2. The *Gremlin* locus was analyzed comparing genomic DNA from wild-type and $ld^{J/J}$ embryos. The genomic region containing the intron–exon 2 boundary was amplified by PCR and PCR products separated on a 1.0% agarose gel, and in all cases (cDNAs and genomic DNAs) only one specific fragment was amplified (data not shown). These amplified DNA bands were cloned and their sequences analyzed using the ClustalW-X program (http://www.ebi.ac.uk/clustalw). Sequences of all primers used for these studies are available upon request.

### Generation of Fmn mutant alleles

The $Fmn^{\Delta 10}$ allele was obtained by successive targeting in R1 ES cells (Nagy et al. 1993). Initially, *Fmn* exon 10 (151 bases) was completely replaced by a PGK-*Neo*^R expression cassette with an SV40 polyadenylation site and a *LoxP* site was inserted further downstream in the intron (Fig. 2B). One of three correctly recombined ES-cell clones was selected for additional gene targeting. A PGK-*Hygro*^R cassette flanked by two *loxP* sites and an *En-2* splice acceptor-IRES-*LacZ* expression cassette (Mountford et al. 1994) was inserted into *Fmn* exon 24 using a *Spe1* site 86 bases downstream of the translational stop codon. Fifty-three correctly targeted ES-cell clones were obtained and characterized extensively by genomic Southern blot analysis to confirm correct alterations of both targeted genomic sites. To identify clones carrying both targeting sites in *cis*, 25 ES-cell clones were electroporated with a *Cre* expression vector. For 14 ES-cell clones, the correct *Cre*-mediated excision patterns were obtained for all possible combinations between the three *LoxP* sites (Fig. 2B). ES-cell clones carrying the $Fmn^{\Delta 10}$ allele were injected into C57BL/6 blastocysts and germ-line transmission was obtained. $Fmn^{\Delta 10}$ mice were maintained by breeding a mixed 129xC57/BL6 background. The $Fmn^{\Delta 10.24}$ allele was generated by intercrossing $Fmn^{\Delta 10/+}$ mice with the *Cre* deleter mouse strain (Schwenk et al. 1995). PCR analysis was used to show that excision had occurred between the two most distant *LoxP* sites, causing deletion of the genomic region spanning *Fmn* exons 10–24 (170 kb).

### RT–PCR analysis of Formin expression

Total RNA from wild-type, $Fmn^{\Delta 10}$, and $Fmn^{\Delta 10.24}$ homozygous embryos was isolated using the RNeasy extraction kit (Qiagen). First strand cDNAs were synthesized according to standard procedures by using 17 µg of total RNA. Subsequently, PCR was performed to detect *Formin* transcripts. The following primer pairs were used: forward primer in exon 9 (e9, 5′-GCTCTTCCTAACAGTGGAGGTCC-3′) and reverse primer in exon 15 (e15, 5′-CACACTCTTCATGTGCAACAA-3′) or exon 23 (e23L1, 5′-CTTTGTCTCCACTTTCTTCTCTGATG TC-3′) for wild-type and $Fmn^{\Delta 10/\Delta 10}$ cDNAs, forward primer in exon 9 and reverse primer in IRES (IRES-1, 5′-GCTTCCTTC ACGACATTCAACAGACC-3′) for $Fmn^{\Delta 10.24/\Delta 10.24}$ cDNAs. PCR products were separated on a 1.0% agarose gel and cloned for sequence analysis and alignment using the ClustalW-X program (http://www.ebi.ac.uk/clustalw).

### Culture of mouse limb buds (trunk cultures) and inhibition of FGF signaling

*Shh* expressing cells were grafted into mouse limb buds (30–33 somites, E10.0–E10.25) cultured as described (Zuniga et al. 1999). Alternatively, FGF signaling was blocked by supplementing the culture medium with 10 µM SU5402 (final concentration), an efficient inhibitor of FGF signal transduction (Mohammadi et al. 1997). SU5402 (Calbiochem) was dissolved in 100% DMSO at 10 mg/mL (stock solution). Experimental controls were treated with an equal concentration of DMSO in culture medium (0.03% final). The SU5402 concentration blocking FGF signaling efficiently was established in pilot experiments and is well within the commonly used range of concentrations. Both grafted and SU5402-treated limb buds were cultured for 14–16 h prior to analysis by in situ hybridization.

### Skeletal preparations, whole mount in situ hybridization and LacZ staining

Skeletal preparations and whole mount in situ hybridization assays were carried out as previously described (Zuniga and

Zeller 1999). β-Galactosidase (LacZ) activity was detected in whole mounts (Knittel et al. 1995) with the following modification: Embryos were stained in the dark at 37°C in 1 mg/mL X-Gal, 0.25 mM K$_3$Fe(CN)$_6$, 0.25 mM K$_4$Fe(CN)$_6$, 0.01% NP40, 0.4 mM MgCl$_2$ in 1× PBS.

*BAC constructs and generation of transient transgenic mouse embryos*

The genomic organization of the *Gremlin* and *Formin* loci and the appropriate BACs were identified using sequences from the Mouse Genome Sequencing Consortium (Waterston et al. 2002) and analyzed with the UCSC Genome Browser (http://genome.ucsc.edu). Mouse BAC clones were obtained from BacPac Resources (Children's Hospital Oakland, USA) and modified by ET recombination as described (Spitz et al. 2003). Construct A was engineered by inserting a *LacZ* reporter gene in frame into the *Gremlin* ORF encoded by BAC RP23-113H17 (Fig. 6A) using a *Zeocin* resistance cassette (Invitrogen). Construct B (Fig. 6B) was obtained by deleting the region between exons 19 and 23 from construct A using a *Kanamycin* resistance cassette. Construct C (Fig. 6C) was generated by targeted replacement of *Fmn* exon 23 and all downstream 3′ sequences from BAC 113H17 by a *LacZ* reporter gene driven by a β-globin minimal promoter (Spitz et al. 2003). This cassette is flanked by 50 bases of BAC DNA sequence, which borders the region to be deleted by homologous recombination. All BAC constructs were injected into the pronucleus of fertilized mouse eggs according to standard procedures (Spitz et al. 2001; Nagy et al. 2002) and embryos were collected during gestational day 10 (E10.5) and analyzed by LacZ staining.

## Acknowledgments

## References

Avsian-Kretchmer, O. and Hsueh, A.J. 2003. Comparative genomic analysis of the eight-membered-ring cystine-knot-containing bone morphogenetic protein (BMP) antagonists. *Mol. Endocrinol.* **18:** 1–12.

Bacchelli, C., Goodman, F.R., Scambler, P.J., and Winter, R.M. 2001. Cenani-Lenz syndrome with renal hypoplasia is not linked to FORMIN or GREMLIN. *Clin. Genet.* **59:** 203–205.

Chao, C.W., Chan, D.C., Kuo, A., and Leder, P. 1998. The mouse formin (Fmn) gene: Abundant circular RNA transcripts and gene-targeted deletion analysis. *Mol. Med.* **4:** 614–628.

Evangelista, M., Zigmond, S., and Boone, C. 2003. Formins: Signaling effectors for assembly and polarization of actin filaments. *J. Cell Sci.* **116:** 2603–2611.

Faustino, N.A. and Cooper, T.A. 2003. Pre-mRNA splicing and human disease. *Genes & Dev.* **17:** 419–437.

Gurrieri, F., Kjaer, K.W., Sangiorgi, E., and Neri, G. 2002. Limb anomalies: Developmental and evolutionary aspects. *Am. J. Med. Genet.* **115:** 231–244.

Haramis, A.G., Brown, J.M., and Zeller, R. 1995. The limb deformity mutation disrupts the SHH/FGF-4 feedback loop and regulation of 5′HoxD genes during limb pattern formation. *Development* **121:** 4237–4245.

Jansen, G., Hazendonk, E., Thijssen, K.L., and Plasterk, R.H. 1997. Reverse genetics by chemical mutagenesis in *Caenorhabditis elegans*. *Nat. Genet.* **17:** 119–121.

Justice, M.J. 2000. Capitalizing on large-scale mouse mutagenesis screens. *Nat. Rev. Genet.* **1:** 109–115.

Khokha, M.K., Hsu, D., Brunet, L.J., Dionne, M.S., and Harland, R.M. 2003. Gremlin is the BMP antagonist required for maintenance of Shh and Fgf signals during limb patterning. *Nat. Genet.* **34:** 303–307.

Knittel, T., Kessel, M., Kim, M.H., and Gruss, P. 1995. A conserved enhancer of the human and murine Hoxa-7 gene specifies the anterior boundary of expression during embryonal development. *Development* **121:** 1077–1088.

Kobielak, A., Pasolli, H.A., and Fuchs, E. 2004. Mammalian formin-1 participates in adherens junctions and polymerization of linear actin cables. *Nat. Cell Biol.* **6:** 21–30.

Leader, B. and Leder, P. 2000. Formin-2, a novel formin homology protein of the cappuccino subfamily, is highly expressed in the developing and adult central nervous system. *Mech. Dev.* **93:** 221–231.

Lettice, L.A., Horikoshi, T., Heaney, S.J., Van Baren, M.J., Van Der Linde, H.C., Breedveld, G.J., Joosse, M., Akarsu, N., Oostra, B.A., Endo, N., et al. 2002. Disruption of a long-range *cis*-acting regulator for Shh causes preaxial polydactyly. *Proc. Natl. Acad. Sci.* **99:** 7548–7553.

Maas, R.L., Zeller, R., Woychik, R.P., Vogt, T.F., and Leder, P. 1990. Disruption of formin-encoding transcripts in two mutant limb deformity alleles. *Nature* **346:** 853–855.

Maas, R.L., Jepeal, L.I., Elfering, S.L., Holcombe, R.F., Morton, C.C., Eddy, R.L., Byers, M.G., Shows, T.B., and Leder, P. 1991. A human gene homologous to the formin gene residing at the murine limb deformity locus: Chromosomal location and RFLPs. *Am. J. Hum. Genet.* **48:** 687–695.

Maas, R., Elfering, S., Glaser, T., and Jepeal, L. 1994. Deficient outgrowth of the ureteric bud underlies the renal agenesis phenotype in mice manifesting the limb deformity (ld) mutation. *Dev. Dyn.* **199:** 214–228.

Mayor, C., Brudno, M., Schwartz, J.R., Poliakov, A., Rubin, E.M., Frazer, K.A., Pachter, L.S., and Dubchak, I. 2000. VISTA: Visualizing global DNA sequence alignments of arbitrary length. *Bioinformatics* **16:** 1046–1047.

Merino, R., Rodriguez-Leon, J., Macias, D., Ganan, Y., Economides, A.N., and Hurle, J.M. 1999. The BMP antagonist Gremlin regulates outgrowth, chondrogenesis and programmed cell death in the developing limb. *Development* **126:** 5515–5522.

Michos, O., Panman, L., Vintersten, K., Beier, K., Zeller, R., and Zuniga, A. 2004. Gremlin mediated BMP antagonism induces the epithelial–mesenchymal feedback signaling controlling metanephric kidney and limb organogenesis. *Development* (in press).

Minabe-Saegusa, C., Saegusa, H., Tsukahara, M., and Noguchi, S. 1998. Sequence and expression of a novel mouse gene PRDC (protein related to DAN and cerberus) identified by a gene trap approach. *Dev. Growth Differ.* **40:** 343–353.

Mohammadi, M., McMahon, G., Sun, L., Tang, C., Hirth, P., Yeh, B.K., Hubbard, S.R., and Schlessinger, J. 1997. Structures of the tyrosine kinase domain of fibroblast growth factor receptor in complex with inhibitors. *Science* **276:** 955–960.

Morgan, B.A., Conlon, F.L., Manzanares, M., Millar, J.B., Kanuga, N., Sharpe, J., Krumlauf, R., Smith, J.C., and Sedgwick, S.G. 1996. Transposon tools for recombinant DNA manipulation: Characterization of transcriptional regulators from yeast, *Xenopus*, and mouse. *Proc. Natl. Acad. Sci.* **93:** 2801–2806.

Morgan, N.V., Bacchelli, C., Gissen, P., Morton, J., Ferrero, G.B., Silengo, M., Labrune, P., Casteels, I., Hall, C., Cox, P., et al. 2003. A locus for asphyxiating thoracic dystrophy, ATD, maps to chromosome 15q13. *J. Med. Genet.* **40:** 431–435.

Mountford, P., Zevnik, B., Duwel, A., Nichols, J., Li, M., Dani, C., Robertson, M., Chambers, I., and Smith, A. 1994. Dicistronic targeting constructs: Reporters and modifiers of mammalian gene expression. *Proc. Natl. Acad. Sci.* **91:** 4303–4307.

Nagy, A., Rossant, J., Nagy, R., Abramow-Newerly, W., and Roder, J.C. 1993. Viable cell culture-derived mice from early passage embryonic stem cells. *Proc. Natl. Acad. Sci.* **90:** 8424–8428.

Nagy, A., Gertsensten, M., Vintersten, K., and Behringer, R. 2002. *Manipulating the mouse embryo: A laboratory manual.* Cold Spring Harbor Press, Cold Spring Harbor, New York.

Niehrs, C. and Pollet, N. 1999. Synexpression groups in eukaryotes. *Nature* **402:** 483–487.

Panman, L. and Zeller, R. 2003. Patterning the limb before and after SHH signalling. *J. Anat.* **202:** 3–12.

Perkins, A.S. 2002. Functional genomics in the mouse. *Funct. Integr. Genomics* **2:** 81–91.

Schwenk, F., Baron, U., and Rajewsky, K. 1995. A cre-transgenic mouse strain for the ubiquitous deletion of loxP-flanked gene segments including deletion in germ cells. *Nucleic Acids Res.* **23:** 5080–5081.

Spitz, F., Gonzalez, F., Peichel, C., Vogt, T.F., Duboule, D., and Zakany, J. 2001. Large scale transgenic and cluster deletion analysis of the HoxD complex separate an ancestral regulatory module from evolutionary innovations. *Genes* & *Dev.* **15:** 2209–2214.

Spitz, F., Gonzalez, F., and Duboule, D. 2003. A global control region defines a chromosomal regulatory landscape containing the HoxD cluster. *Cell* **113:** 405–417.

Sun, X., Mariani, F.V., and Martin, G.R. 2002. Functions of FGF signalling from the apical ectodermal ridge in limb development. *Nature* **418:** 501–508.

Vogt, T.F., Jackson Grusby, L., Wynshaw Boris, A.J., Chan, D.C., and Leder, P. 1992. The same genomic region is disrupted in two transgene-induced limb deformity alleles. *Mamm. Genome* **3:** 431–437.

Wang, C.C., Chan, D.C., and Leder, P. 1997. The mouse formin (Fmn) gene: Genomic structure, novel exons, and genetic mapping. *Genomics* **39:** 303–311.

Waterston, R.H., Lindblad-Toh, K., Birney, E., Rogers, J., Abril, J.F., Agarwal, P., Agarwala, R., Ainscough, R., Alexandersson, M., An, P., et al. 2002. Initial sequencing and comparative analysis of the mouse genome. *Nature* **420:** 520–562.

Woychik, R.P., Stewart, T.A., Davis, L.G., D'Eustachio, P. and Leder, P. 1985. An inherited limb deformity created by insertional mutagenesis in a transgenic mouse. *Nature* **318:** 36–40.

Woychik, R.P., Generoso, W.M., Russell, L.B., Cain, K.T., Cacheiro, N.L.A., Bultman, S.J., Selby, P.B., Dickinson, M.E.,

Hogan, B.L.M., and Rutledge, J.C. 1990. Molecular and genetic characterisation of a radiation-induced structural rearrangement in mouse chromosome 2 causing mutations at the limb deformity and agouti loci. *Proc. Natl. Acad. Sci.* **87:** 2588–2592.

Wynshaw-Boris, A., Ryan, G., Deng, C.X., Chan, D.C., Jackson-Grusby, L., Larson, D., Dunmore, J.H., and Leder, P. 1997. The role of a single formin isoform in the limb and renal phenotypes of limb deformity. *Mol. Med.* **3:** 372–384.

Zákány, J. and Duboule, D. 1996. Synpolydactyly in mice with a targeted deficiency in the *HoxD* complex. *Nature* **384:** 69–71.

Zeller, R. and Deschamps, J. 2002. Developmental biology: First come, first served. *Nature* **420:** 138–139.

Zeller, R., Haramis, A., Zuniga, A., McGuigan, C., Dono, R., Davidson, G., Chabanis, S., and Gibson, T. 1999. *Formin* defines a large family of morphoregulatory genes and functions in establishment of the polarising region. *Cell Tissue Res.* **296:** 85–93.

Zuniga, A. and Zeller, R. 1999. Gli3 (Xt) and formin (ld) participate in the positioning of the polarising region and control of posterior limb-bud identity. *Development* **126:** 13–21.

Zuniga, A., Haramis, A.P., McMahon, A.P., and Zeller, R. 1999. Signal relay by BMP antagonism controls the SHH/FGF4 feedback loop in vertebrate limb buds. *Nature* **401:** 598–602.

# Mouse *limb deformity* mutations disrupt a global control region within the large regulatory landscape required for *Gremlin* expression

Aimée Zuniga, Odyssé Michos, François Spitz, et al.

| | |
|---|---|
| **Supplemental Material** | http://genesdev.cshlp.org/content/suppl/2004/06/16/299904.DC1 |
| **References** | This article cites 42 articles, 14 of which can be accessed free at: http://genesdev.cshlp.org/content/18/13/1553.full.html#ref-list-1 |
| **License** | |
| **Email Alerting Service** | Receive free email alerts when new articles cite this article - sign up in the box at the top right corner of the article or  **click here.** |